Polymer Testing 83 (2020) 106353

Contents lists available at ScienceDirect

Polymer Testing

journal homepage: http://www.elsevier.com/locate/polytest

Test Method

Measurement of viscoelastic properties for polymers by nanoindentation

Yuemin Wang [a], Lei Shang [a], Panpan Zhang [b], Xiangqiao Yan [a], Ke Zhang [c], Shuliang Dou [a,**], Jiupeng Zhao [c,***], Yao Li [a,*]

[a] Center for Composite Materials and Structures, Harbin Institute of Technology, Harbin, China
[b] Jincheng Campus, Taiyuan University of Science and Technology, Jincheng, China
[c] School of Chemistry and Chemical Engineering, Harbin Institute of Technology, Harbin, China

A R T I C L E I N F O

Keywords:
Nanoindentation
Viscoelasticity
Creep compliance
Relaxation modulus
Prony series

A B S T R A C T

A new method has been proposed and verified to measure the viscoelastic properties of polymers by nanoindentation tests. With the mechanical response of load–displacement curves at different loading rates, the parameters of creep compliance and relaxation modulus are calculated through the viscoelastic contact model. Dynamic thermomechanical analysis (DMA) tests are conducted to compare the results by the proposed technique. The results show that the correlation coefficients between DMA tests and the new method are above 0.9 in the entire range, which verified the feasibility of the method. The loading curves fitted by the model are identical to the experimental curves within the discrete points and so it shows that this technique is more suitable for general linear viscoelastic materials. Numerical creep tests are carried out to examine the effectiveness of the proposed method by input the Prony series calculated by the three-element Maxwell model and the viscoelastic contact model. The good agreement shows that the proposed technique can be applied in practice.

1. Introduction

With the increasing use of very small structures, nanocomposites, and other micromaterials in various engineering areas such as optic, mechanical, electric, and microelectromechanical systems, a critical evaluation of the mechanical behavior is needed to predict the reliability of such materials [1–5]. Traditional mechanical testing is not suitable for small-scale or local performance testing due to the limitations of sample size, experimental conditions, and test resolution [6–10]. Nanoindentation has become one of the most important methods for small-scale measurement because of its advantages of high resolution, simple sample preparation, and nondestructive testing [11–15]. For general materials, the nanoindentation test can easily acquire hardness and elastic modulus, and, more importantly, in the plastic region, the inversion calculation of constitutive relation can be carried out by dimensional analysis [16–18]. However, for time-dependent materials, the viscoelastic parameters cannot be directly measured, and the inversion calculation method proposed by previous researchers is not suitable, so there is a need to explore how to obtain the mechanical properties of viscoelastic materials. Unfortunately, there are few studies on the calculation of viscoelastic parameters using nanoindentation.

Wei et al. [19] proposed a combination of one dashpot in series with 1 K model and 2 K models with distinct time constants in series to describe the deformation of polymers under indentation tests. A coupled experimental/numerical approach for the characterization of the local mechanical behavior of epoxy polymer materials was proposed by Minervino et al. They found that the pure viscoelastic constitutive law cannot reproduce the local polymer behavior and needs to be enhanced by adding material-softening behavior [20]. Menčík et al. [21] proposed a model consisting of spring, plastic element, dashpot, and 2 K–Voigt bodies to calculate the load response of viscoelastic-plastic materials, including biological and restorative biomaterials. Some other models for viscoelastic polymers have been proposed as well [22–27]. Although efforts have been made to explain the viscoelastic properties of polymers, the models suggested in the previous studies are either very complex, resulting in time-consuming calculations, or based on complex input data, such as complex loading profiles. In addition, the parameters obtained cannot be directly applied to engineering mechanical calculations, especially for simulation calculations.

The paper proposes and validates a method to directly calculate

* Corresponding author.
** Corresponding author.
*** Corresponding author.
E-mail addresses: dousl@hit.edu.cn (S. Dou), jpzhao@hit.edu.cn (J. Zhao), yaoli@hit.edu.cn (Y. Li).

https://doi.org/10.1016/j.polymertesting.2020.106353
Received 10 September 2019; Received in revised form 6 January 2020; Accepted 14 January 2020
Available online 20 January 2020
0142-9418/

viscoelastic parameters using nanoindentation tests. Polyimide (PI) thin film was used to validate this method. The method can acquire creep compliance and relaxation modulus based on nanoindentation experiments at different loading rates. For comparison, dynamical mechanical analysis (DMA) creep experiments were carried out, and then the viscoelastic parameters were fitted by the generalized Kelvin/Maxwell model, so that they could be used to compare with the results of the nanoindentation method. Finally, Prony series calculated by the two methods were used in the creep simulation to verify the method.

2. Theoretical background

The nanoindentation test can be regarded as a process in which a rigid indenter is gradually pressed into an elastic half-space (Supporting Information Section I). For a conical indenter, the relationship between load and displacement can be obtained by the Sneddon contact model [28,29]:

$$P = \frac{4}{\pi(1-\upsilon)\tan\alpha} G h^2 \tag{1}$$

where P is the indentation load, h is the indentation depth, G is the shear modulus and $G = E/2(1+\upsilon)$, E is the elastic modulus, υ is Poisson's ratio, and α is the angle of the indenter.

Similarly, according to this line of thought, when testing viscoelastic materials, the experimental process can be regarded as a quasi-static boundary issue between rigid indenter and semi-infinite space materials with time dependence (Supporting Information Section II). The difference between them is that viscoelastic materials have creep or relaxation characteristics due to their time-dependence properties, and can cause the moving boundary problem. Therefore, how to introduce time variables into the contact model is a key question. The load-displacement curve involves time factors such as loading rate, holding time, unloading rate, etc. In this paper, loading rate was used to express time variables.

According to Riande's research [30], the hereditary integral operator introduced into Equation (1) leads to the relationship between displacement and load:

$$h^2(t) = \frac{\pi(1-\nu)\tan\alpha}{4} \int_0^t J(t-\tau)\left[\frac{dp(\tau)}{d\tau}\right] d\tau \tag{2}$$

where $J(t)$ is the creep compliance function in shear, t is the time variable, and τ is the retardation time in the model.

The indentation load can be shown as $P(t) = \upsilon_0 t H(t)$ by the constant loading rate, where υ_0 is the loading rate and $H(t)$ is the Heaviside step function. Substituting $P(t)$ into Equation (2), we have

$$h^2(t) = \frac{\pi(1-\nu)\nu_0 \tan\alpha}{4} \int_0^t J(t-\tau) d\tau \tag{3}$$

Differentiating Equation (3) with respect to t, we have

$$J(t) = \frac{8h}{\pi(1-\nu)\tan\alpha} \frac{dh}{dp} \tag{4}$$

The general representation of creep compliance based on the Kelvin model is

$$J(t) = J_0 + \sum_{i=1}^{N} J_i\left(1 - e^{-t/\tau_i}\right) \tag{5}$$

where $J_0, J_1, J_2, \ldots J_n$ are compliance numbers, $\tau_1, \tau_2, \ldots \tau_n$ are retardation times, and N is a positive integer.

Similarly, the general representation of the relaxation modulus based on the Maxwell model is

$$E(t) = E_0 + \sum_{i=1}^{N} E_i e^{-t/\tau_i} \tag{6}$$

where $E_0, E_1, E_2, \ldots E_n$ are relaxation modulus numbers, $\tau_1, \tau_2, \ldots \tau_n$ are retardation times, and N is a positive integer.

Substituting Equation (5) into Equation (4), we have

$$h^2\left(t\right) = \frac{1}{4}\pi\left(1-\nu\right)\tan\alpha\left[\left(J_0 + \sum_{i=1}^{N} J_i\right)P\left(t\right) - \sum_{i=1}^{N} J_i \nu_0 \tau_i\left(1 - e^{-P(t)/(\nu_0\tau_i)}\right)\right] \tag{7}$$

Equation (7) is the viscoelastic contact model based on nanoindentation. Applying the nanoindentation experiment at different loading rates, the relationship between loads and displacement squares can be obtained, and different creep parameters can be fitted. Therefore, the equation can analyze the viscoelastic relationship of time-dependent materials. According to the Laplace transformation, there is a conversion relationship between creep compliance and relaxation modulus in the Laplace domain, as shown in Equation (8), hence the relaxation modulus can be obtained by creep compliance [30,31]:

$$E\left(t\right) = L^{-1}\left\{\widetilde{E}\left(s\right)\right\} = L^{-1}\left(\frac{1}{s^2\widetilde{J}(s)}\right) \tag{8}$$

where $E(t)$ is the relaxation modulus, $L\{\}$ is the Laplace operator, s is the Laplace variable, $\widetilde{J}(s)$ and $\widetilde{E}(s)$ are the functions obtained by Laplace transformation, and $\widetilde{J}(s)\widetilde{E}(s) = 1/s^2$.

3. Experiments

A commercial polyimide (PI) thin film (CENPI, Ningbo, CHN) was adopted in our study. The specimen surface was cleaned ultrasonically several times and all specimens were aged for approximately 48 h before nanoindentation tests. Samples of 15 × 10 × 0.05 mm size were directly glued onto a metallic holder to perform the nanoindentation tests. The tests were performed with a nanoindenter (Keysight G200) provided with continuous stiffness measurement (CSM). A Berkovich diamond tip was employed and all experiments were performed at room temperature (20 °C). Nanoindentation experiments were carried out in a stress-loading manner with constant loading of 10 mN. Five fixed loading rates of 2, 1, 0.5, 0.1 and 0.05 mN/s were tested. For each sample, at least five tests were conducted to calculate the average value of the mechanical parameters.

Similarly, after the surface cleaning, samples of 30 × 10 × 0.05 mm size were prepared by mechanical cutting for DMA creep tests. The creep tests of PI film were performed with film tension mode using a DMA Q800 dynamic mechanical analyzer (TA Instruments, New Castle, DE, USA). The DMA tests were performed under controlled stress. In order to improve the accuracy of the tests, a preliminary test was carried out at room temperature with constant stress equal to 0.1 MPa. Immediately after the preliminary test, the samples were kept for 30 min at the test temperature (20 °C). The initial stress was 5 MPa. When the stress reached the setting point, the value of strain with time change was recorded, and then the creep curves were obtained.

4. Results and discussion

The load-displacement curves by nanoindentation experiments are shown in Fig. 1. It can be seen that when the maximum load has the same value, different maximum displacement appears. It is worth noting that when the loading rate becomes larger, the curves obtained by the experiment are statistically insignificant with each other. The differences of the maximum force measured from nanoindentation with the loading rates of 0.5, 1 and 2 mN/s are below 5%.With the loading rate decreasing, the load-displacement curve begins to discrete. This is because the polyimide thin film is a type of viscoelastic material, which is time-dependent. Therefore, the loading time increases when the loading rate decreases, and then lead to the increase of creep value. It means that the creep phenomenon is more pronounced during the low

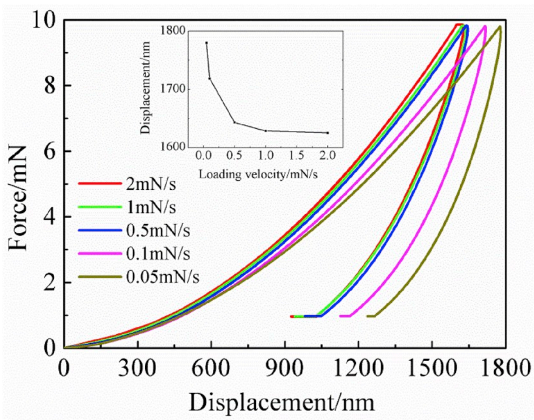

Fig. 1. Load-displacement curves for polyimide (PI) materials by nanoindentation under different loading rates.

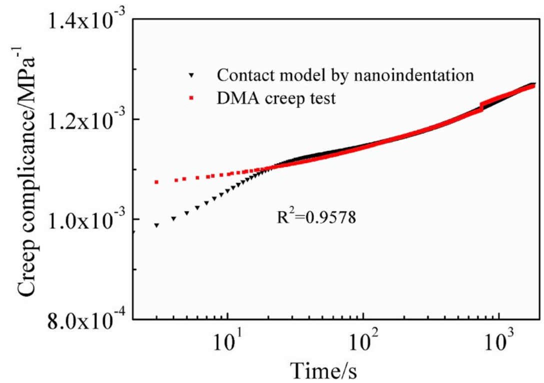

Fig. 2. The comparison of creep compliance between the contact model and DMA test.

loading rate, which has also been observed in other studies [32–34].

According to the nanoindentation test and the viscoelastic contact model using Equation (7), the relationship between $h^2(t)$ and $P(t)$ under different loading rates can be obtained, as well as the creep compliance.

Because the angle between the indenter and the measured material plane is 19.7°, Equation (7) can be simplified as follows:

$$h^2\left(t\right) = 0.1883\left[\left(J_0 + \sum_{i=1}^{N} J_i\right)P\left(t\right) - \sum_{i=1}^{N} J_i v_0 \tau_i \left(1 - e^{-P(t)/(v_0\tau_i)}\right)\right] \tag{9}$$

The data of load-displacement curves at five loading rates are introduced into Equation (9) for fitting calculation and then the relevant parameters for calculating creep compliance can be obtained, as shown in Table 1.

Substituting parameters in Table 1 into Equation (5), the function of creep compliance for polyimide film can be deduced:

$$J(t) = 0.0009397 + 0.0001712\left(1 - e^{-t/9.23}\right) + 0.00003104\left(1 - e^{-t/86.21}\right) + 0.0001534\left(1 - e^{-t/1000}\right) \tag{10}$$

Fig. 2 shows a comparison of creep compliance between the viscoelastic contact model and DMA creep experiments. The correlation coefficient is 0.9578 in the entire range. It can be concluded that the two curves have the similar development trend and good fitting degree over time. Note that, at the early creep stage (∼ = 15s), the creep compliance obtained by DMA creep experiment is slightly higher than that obtained by viscoelastic contact model, and the maximum difference is 7.6%. The viscoelastic contact model is based on the Herz model that requires an ideal contact between the two solids. Thus, the deviation observed at the early stage is likely caused by the thermal drift or size effect [14,16]. Although the slight difference at the early stage, as the creep time increases, they are basically the same in the overall rage (Supporting Information). It proves that the viscoelastic contact model based on nanoindentation is reasonable and the creep compliance calculated by the nanoindentation experiment is feasible.

The parameters in Table 1 are re-introduced into Equation (9) to obtain the relationship between load and displacement at different loading rates. When the loading rate is 2 mN/s, we can get

$$h^2(t) = 0.1883\left[0.0012953P(t) - 0.00319\left(1 - e^{-P(t)/18.46}\right) - 0.0054\left(1 - e^{-P(t)/172.42}\right) - 0.3068\left(1 - e^{-P(t)/2000}\right)\right] \tag{11}$$

Similarly, equations for other loading rates can be obtained in this manner, and the relevant parameters are shown in Table 2.

The fitted loading curve can be inverted by parameters in Table 2, and then compared with the nanoindentation experiment, as shown in Fig. 3. It can be seen that the correlation coefficients between the two sets of data are all above 0.95 within the discrete points, which verifies the validity of the function based on nanoindentation. And with the increased loading rate, the positions of discrete points in the loading curve are larger concomitantly, as shown in Fig. 3f. However, it can also be seen that with the increased indent displacement, the fitted curves and experimental curves have certain discrete deviation.

In this paper, as an approximation, we use discrete points as the limit of linearity for polyimide thin film. As mentioned in Section 2, the viscoelastic contact model in this paper is based on Hertz contact and a quasi-static boundary value problem with moving boundary [35,36]. This requires that the area of contact is small compared with the dimensions of the bodies and small strains are assumed. Moreover, both bodies in contact are linearly viscoelastic, and the material properties can be characterized by creep or relaxation functions. In fact, the indentation process of nanoindentation is three-dimensional nonlinear mechanical behavior and can induce deformations in both the linear and nonlinear viscoelastic regimes. If the indentation load or depth is small, indentation on a viscoelastic half-space can be considered as a linear viscoelastic problem. Therefore, the function proposed in this paper is applicable to shallow indent experiments of nanodentation, and with the increased indentation depth, the nonlinear contact model may be developed.

According to Equation (8), the calculated creep compliance can be converted into a relaxation modulus, we can get

$$E(t) = 775 + 104.4e^{-t/20} + 40.85e^{-t/200} + 76.44e^{-t/1200} \tag{12}$$

Similarly, creep compliance calculated by the DMA experiment can be transformed for the relaxation modulus. By introducing the parameters into the three-element generalized Maxwell model (Supporting Information), the equation can be obtained:

$$E(t) = 771.4 + 45.93e^{-t/20} + 45.58e^{-t/300} + 76.67e^{-t/1200} \tag{13}$$

Fig. 4 shows a comparison of relaxation modulus between the three-

Table 1
Parameters for calculating creep compliance.

Parameter	J_0/MPa^{-1}	J_1/MPa^{-1}	J_2/MPa^{-1}	J_3/MPa^{-1}	τ_1/s	τ_2/s	τ_3/s
Value	9.397e-04	1.712e-4	3.104e-5	1.534e-4	9.23	86.21	1000

Table 2
Parameters of relationship between $h^2(t)$ and $P(t)$.

Loading rate υ_0	$J_0+\sum_{i=1}^{3} J_i$	$J_1\upsilon_0\tau_1$	$J_2\upsilon_0\tau_2$	$J_3\upsilon_0\tau_3$	$\upsilon_0\tau_1$	$\upsilon_0\tau_2$	$\upsilon_0\tau_3$
2 mN/s	1.2953e-3	3.19e-3	5.4e-3	0.3068	18.46	172.42	2000
1 mN/s	1.2953e-3	1.596e-3	2.7e-3	0.1534	9.32	86.21	1000
0.5 mN/s	1.2953e-3	7.98e-4	1.35e-3	0.0766	4.66	43.105	500
0.1 mN/s	1.2953e-3	1.596e-4	2.7e-4	0.01532	0.932	8.621	100
0.05 mN/s	1.2953e-3	7.98e-5	1.35e-4	7.66e-3	0.456	4.315	50

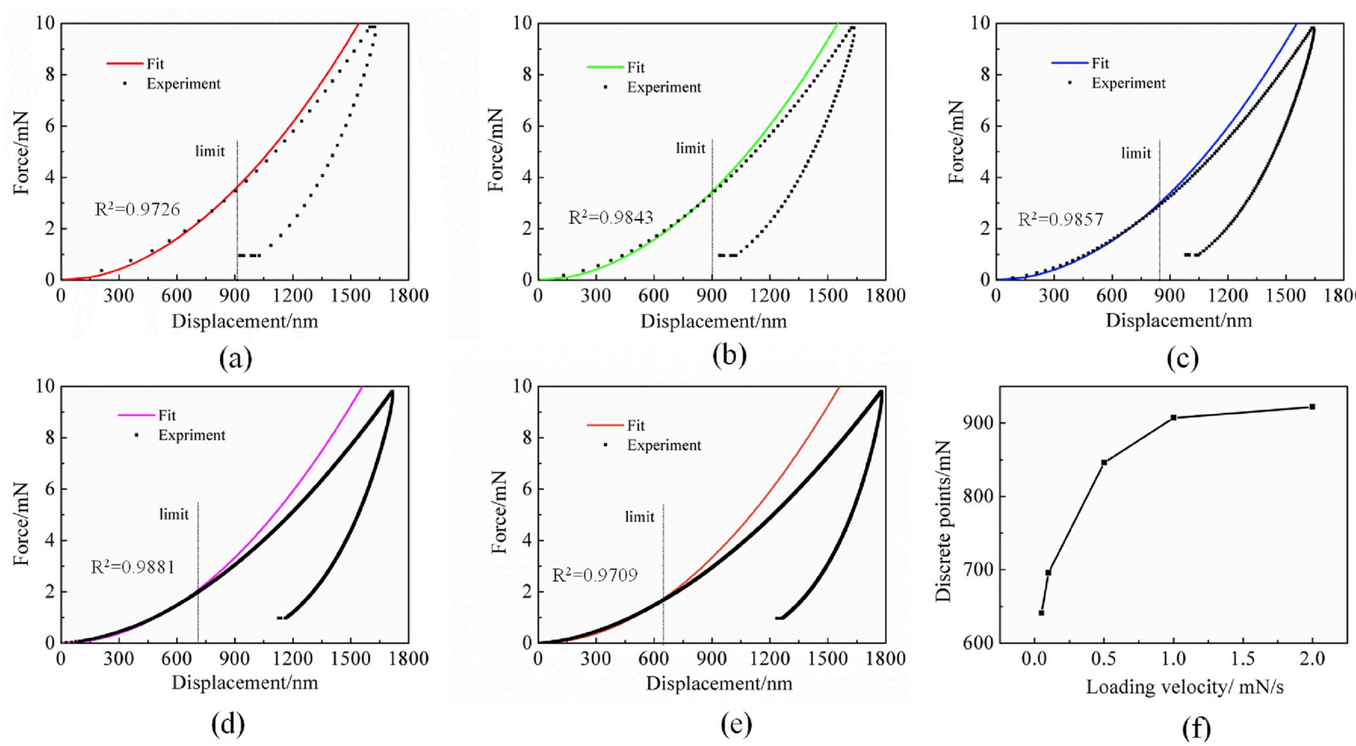

Fig. 3. Fitting curves and discrete points at different loading rates: (**a**) 2 mN/s, (**b**) 1 mN/s, (**c**) 0.5 mN/s, (**d**) 0.1 mN/s, (**e**) 0.05 mN/s; and (**f**) discrete points at different loading velocities.

element Maxwell model and the viscoelastic contact model. Similar to Fig. 2, the deviation at the early relaxation stage (∼ = 30 s) is observed in the curves. This is also likely caused by reasons mentioned in the creep phenomenon. The maximum difference between two set of data is 4.9%, and the correlation coefficients is 0.9011. With the time increased, the two types of data have a good fitting degree in the overall range (Supporting Information). It can also prove the method proposed in this paper.

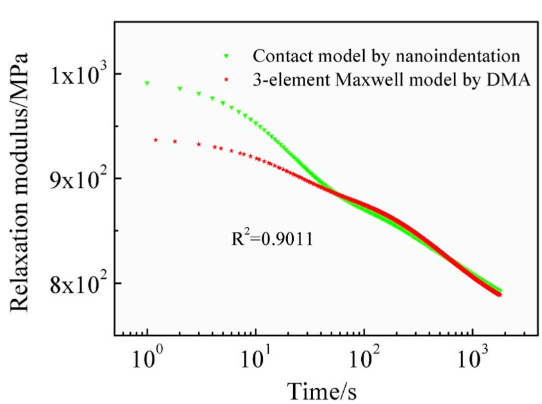

Fig. 4. Curves of relaxation modulus by the three-element Maxwell model and viscoelastic contact model.

To conclude, the viscoelastic contact model based on nanoindentation can calculate both the relaxation modulus and creep compliance. The calculated results are basically consistent with the traditional experiments, it provide a new method to acquire viscoelastic properties.

5. FEM simulation

In order to further verify the viscoelastic parameters obtained by nanoindentation, FEM was used to simulate a creep test. All simulation studies were performed using the commercial finite element software Abaqus version 6.11 (Dassault Systems, France). The same size sample as the DMA test was selected to establish the geometric model, as shown in Fig. 5. In this model, a three-dimensional C3D8R element and hexahedral mesh were used. One end of the finite element geometric model was fully constrained and the opposite side had initial stress imposed without constraint for other aspects.

The simulation was carried out in two steps. The first step was quasi-static loading with the purpose of exerting initial stress; the second step was viscous loading, keeping the initial stress for 30 min, and observing the occurrence of creep phenomenon in this time range. The parameters input to the model were Prony series converted by the creep compliance, as shown in Table 3.

Fig. 6 shows the creep results between the simulations by two types

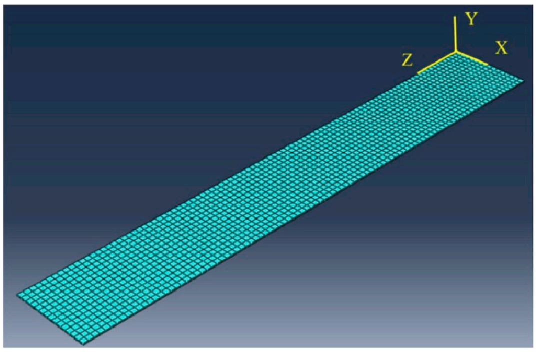

Fig. 5. Simulated geometric model of PI thin film.

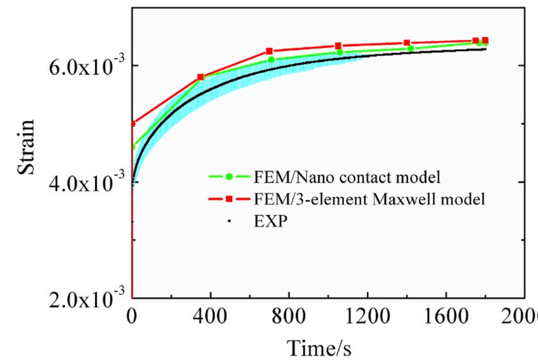

Fig. 6. Comparison of simulation results under three types of viscoelastic parameters.

Table 3
Prony series calculated by two methods.

Prony series	DMA test	Nanoindentation
$G_1 = K_1$	0.0489	0.1047
$G_2 = K_2$	0.0485	0.0410
$G_3 = K_3$	0.0816	0.0767

of Prony series and the traditional experiment. It can be seen that the simulation curves obtained by the two methods are consistent with the experimental curves of DMA in the overall time, which verifies the accuracy of the method. The experimental data curves are slightly lower than the simulated data curves. The maximum difference is 15% between the simulations and the DMA tests, which is mainly caused by the precision and astringency of the algorithm of the simulation. And the maximum difference between two types of Prony series is 9.2%, respectively. With the time increased, the three type's curves have a good fitting degree in the entire range. It is further proved that the viscoelastic contact model based on nanoindentation can be applied to polyimide materials, and it also provides a calculation method for other viscoelastic polymers.

6. Conclusion

A new technique for measuring viscoelastic parameters based on nanoindentation has been proposed and validated. Creep compliance and relaxation modulus are calculated through the viscoelastic contact model by nanoindentation experiments at different loading rates. The correlation coefficient between curves by the proposed method and DMA experiment is 0.9578 for creep compliance and 0.9011 for relaxation modulus, respectively, which confirmed the rationality of the method. Loading curves fitted by the proposed model at five different rates are basically consistent with the nanoindentation experiments before the discrete points. The discrete phenomenon appears when the indentation depth is large, which indicates that the method is expected to be applicable to general linear viscoelastic materials. Based on the Prony series of the generalized Kelvin/Maxwell model, numerical simulation are conducted, further confirmed the feasibility of this method and providing a new idea for viscoelastic polymer materials at a small scale.

Declaration of competing interest

We declare that we do not have any commercial or associative interest that represents a conflict of interest in connection with the work submitted.

CRediT authorship contribution statement

Yuemin Wang: Conceptualization, Methodology, Writing - original draft. **Lei Shang:** Software, Writing - original draft. **Panpan Zhang:** Visualization, Investigation. **Xiangqiao Yan:** Supervision, Conceptualization. **Ke Zhang:** Validation. **Shuliang Dou:** Project administration, Writing - review & editing. **Jiupeng Zhao:** Writing - review & editing. **Yao Li:** Supervision, Validation, Funding acquisition.

Appendix A. Supplementary data

Supplementary data to this article can be found online at https://doi.org/10.1016/j.polymertesting.2020.106353.

References

[1] A.M. Díez-Pascual, M.A. Gómez-Fatou, F. Ania, et al., Nanoindentation in polymer nanocomposites, Prog. Mater. Sci. 67 (2015) 1–94.
[2] R.F. Gibson, A review of recent research on nanoindentation of polymer composites and their constituents, Compos. Sci. Technol. 105 (2014) 51–65.
[3] G.Z. Voyiadjis, L. Malekmotiei, A. Samadi-Dooki, Indentation size effect in amorphous polymers based on shear transformation mediated plasticity, Polymer 137 (2018) 72–81.
[4] B.G. Yoo, I.C. Choi, Y.J. Kim, et al., Room-temperature anelasticity and viscoplasticity of Cu–Zr bulk metallic glasses evaluated using nanoindentation, Mater. Sci. Eng. A 577 (2013) 101–104.
[5] G.Z. Voyiadjis, L. Malekmotiei, Variation of the strain rate during CSM nanoindentation of glassy polymers and its implication on indentation size effect, J. Polym. Sci. B Polym. Phys. 54 (21) (2016) 2179–2187.
[6] W. He, P. Goudeau, E. Le Bourhis, et al., Study on Young's modulus of thin films on Kapton by microtensile testing combined with dual DIC system, Surf. Coat. Technol. 308 (2016) 273–279.
[7] J. Giró-Paloma, J.J. Roa, A.M. Díez-Pascual, et al., Depth-sensing indentation applied to polymers: a comparison between standard methods of analysis in relation to the nature of the materials, Eur. Polym. J. 49 (12) (2013) 4047–4053.
[8] R. Martinez, L.R. Xu, Comparison of the Young's moduli of polymers measured from nanoindentation and bending experiments, MRS Commun. 4 (3) (2014) 89–93.
[9] V. Tvergaard, A. Needleman, Polymer indentation: numerical analysis and comparison with a spherical cavity model, J. Mech. Phys. Solids 59 (9) (2011) 1669–1684.
[10] O. Das, A.K. Sarmah, D. Bhattacharyya, Nanoindentation assisted analysis of biochar added biocomposites, Compos. B Eng. 91 (2016) 219–227.
[11] C. Jin, D.M. Ebenstein, Nanoindentation of compliant materials using Berkovich tips and flat tips, J. Mater. Res. 32 (2) (2017) 435–450.
[12] Y. Yang, Sensitivity of nanoindentation strain rate in poly (ester-ester-ketone) using atomic force microscopy, Polym. Test. 53 (2016) 85–88.
[13] T. Jin, X. Niu, G. Xiao, et al., Effects of experimental variables on PMMA nano-indentation measurements, Polym. Test. 41 (2015) 1–6.
[14] G. Feng, A.H.W. Ngan, Effects of creep and thermal drift on modulus measurement using depth-sensing indentation, J. Mater. Res. 17 (3) (2002) 660–668.
[15] P. Frontini, S. Lotfian, M.A. Monclús, et al., High temperature nanoindentation response of RTM6 epoxy resin at different strain rates, Exp. Mech. 55 (5) (2015) 851–862.
[16] W.C. Oliver, G.M. Pharr, An improved technique for determining hardness and elastic modulus using load and displacement sensing indentation experiments, J. Mater. Res. 7 (6) (1992) 1564–1583.
[17] N. Chollacoop, M. Dao, S. Suresh, Depth-sensing instrumented indentation with dual sharp indenters, Acta Mater. 51 (13) (2003) 3713–3729.
[18] M. Dao, N. Chollacoop, K.J. Van Vliet, et al., Computational modeling of the forward and reverse problems in instrumented sharp indentation, Acta Mater. 49 (19) (2001) 3899–3918.

[19] P.J. Wei, W.X. Shen, J.F. Lin, Analysis and modeling for time-dependent behavior of polymers exhibited in nanoindentation tests, J. Non-Cryst. Solids 354 (33) (2008) 3911–3918.

[20] M. Minervino, M. Gigliotti, M.C. Lafarie-Frenot, et al., A coupled experimental/numerical approach for the modelling of the local mechanical behaviour of epoxy polymer materials, J. Mech. Phys. Solids 67 (2014) 129–151.

[21] J. Menčík, L.H. He, M.V. Swain, Determination of viscoelastic–plastic material parameters of biomaterials by instrumented indentation, J. Mech. Behav. Biomed. Mater. 2 (4) (2009) 318–325.

[22] R. Seltzer, Y.W. Mai, Depth sensing indentation of linear viscoelastic–plastic solids: a simple method to determine creep compliance, Eng. Fract. Mech. 75 (17) (2008) 4852–4862.

[23] R. Song, A.H. Muliana, A. Palazotto, An empirical approach to evaluate creep responses in polymers and polymeric composites and determination of design stresses, Compos. Struct. 148 (2016) 207–223.

[24] M. Zhai, G.B. McKenna, Viscoelastic modeling of nanoindentation experiments: a multicurve method, J. Polym. Sci. B Polym. Phys. 52 (9) (2014) 633–639.

[25] E.G. Herbert, P.S. Phani, K.E. Johanns, Nanoindentation of viscoelastic solids: a critical assessment of experimental methods, Curr. Opin. Solid State Mater. Sci. 19 (6) (2015) 334–339.

[26] G.L. Oliveira, C.A. Costa, S.C.S. Teixeira, et al., The use of nano-and micro-instrumented indentation tests to evaluate viscoelastic behavior of poly (vinylidene fluoride)(PVDF), Polym. Test. 34 (2014) 10–16.

[27] W. Xia, J. Song, D.D. Hsu, et al., Understanding the interfacial mechanical response of nanoscale polymer thin films via nanoindentation, Macromolecules 49 (10) (2016) 3810–3817.

[28] I.N. Sneddon, The relation between load and penetration in the axisymmetric Boussinesq problem for a punch of arbitrary profile, Int. J. Eng. Sci. 3 (1) (1965) 47–57.

[29] Y.T. Cheng, C.M. Cheng, General relationship between contact stiffness, contact depth, and mechanical properties for indentation in linear viscoelastic solids using axisymmetric indenters of arbitrary profiles, Appl. Phys. Lett. 87 (11) (2005) 111914.

[30] E. Riande, R. Diaz-Calleja, M. Prolongo, et al., Polymer Viscoelasticity: Stress and Strain in Practice, CRC Press, 1999.

[31] A. Hernandez-Jimenez, J. Hernandez-Santiago, A. Macias-Garcıa, et al., Relaxation modulus in PMMA and PTFE fitting by fractional Maxwell model, Polym. Test. 21 (3) (2002) 325–331.

[32] Y.J. Lee, J.M. Huang, S.W. Kuo, et al., Low-dielectric, nanoporous polyimide films prepared from PEO–POSS nanoparticles, Polymer 46 (23) (2005) 10056–10065.

[33] T. Crochon, C. Li, M. Lévesque, On time–temperature-dependent viscoelastic behavior of an amorphous polyimide, Mech. Time-Dependent Mater. 19 (3) (2015) 305–324.

[34] R. Xia, H. Zhou, R. Wu, et al., Nanoindentation investigation of temperature effects on the mechanical properties of nafion® 117, Polymers 8 (9) (2016) 344.

[35] E.H. Lee, J.R.M. Radok, The contact problem for viscoelastic bodies, J. Appl. Mech. 27 (3) (1960) 438–444.

[36] W.H. Yang, The contact problem for viscoelastic bodies, J. Appl. Mech. 33 (2) (1966) 395–401.